Autoradiographic Evaluation of Monoclonal Antibodies' Access to Melanoma-Associated Antigens in Melanoma Xenografts

Siegfried Matzku, Jörg Schmid, and Wolfgang Tilgen

Institute of Radiology and Pathophysiology (SM, JS), German Cancer Research Center, and Department of Dermatology (WT), University of Heidelberg, Heidelberg, F.R.G.

Autoradiography of nude mice bearing human malignant melanoma xenografts was performed to characterize the distribution pattern of radioiodinated anti-melanoma monoclonal antibodies (MoAb) and fragments in macroscopic tumor nodules. Non-uniformity of radioactivity distribution was seen in all MoAb-xenograft combinations. The predominant patterns were marked deposition of radioactivity either in the periphery of nodules or in sharply delimited intra-tumoral foci. These patterns were generated by limitations in the accessibility of melanoma tissue rather than gross necrosis or heterogeneity of antigen expression. Computer-aided densitometry of autoradiograms was used to elaborate the difference of accumulation in intra-tumoral hot spots versus cold areas. It was found that increasing uniformity was achieved by increasing the dose of MoAb (i.e., intact IgG) injected, whereas a reduction in the size of MoAb (IgG > $F(ab')_2$ > Fab) showed no such effect. *J Invest Dermatol 95:671–676, 1990*

Diagnostic tumor targeting with MoAb, and even more so immunotherapy with antibody conjugates, ideally requires antibody binding to every tumor cell in a given nodule with saturation of all available binding sites. To control the extent of MoAb binding, methods are needed that would give an overview of the whole tumor at a resolution allowing for single-cell identification. Until now, this problem was approached by two opposing versions of autoradiography. With macro-autoradiography [1], the x-ray film is exposed to large-size tissue sections; the resulting autoradiographs give an overview of a tumor in cross-section and a comprehensive image of radioactivity distribution in normal tissues of rodent hosts. In microscopic autoradiography, small sections of individual tissues are dipped into photographic emulsion. Silver grains are developed above the histologic structures, giving a more precise image of radioactivity associated with cellular and extra-cellular structures. However, an overview of macroscopic tissue areas may hardly be obtained and information as to the rest of the body is not directly accessible.

The initial impetus to our study was given by the observation that antigen densities on cultured melanoma cells did not allow for a prediction of uptake levels in vivo [2], suggesting that additional parameters might have determined gross accumulation in solid melanoma tissue. To get further insight, we analyzed MoAb distribution in xenotransplanted nude mice by autoradiography, with special emphasis on the intra-tumoral accumulation patterns. This comprised nine anti-melanoma MoAb labeled with three different nuclides and six melanoma lines. Starting from this broad basis of evidence, an in-depth examination was carried out with two melanoma lines (i.e., MeWo and MML-I) and the respective MoAb (i.e., M.2.9.4 and HD-Mel 3) were labeled exclusively with ^{125}I. This setup allowed us to best visualize the prototype accumulation patterns observed in melanoma and is the topic of the present report. Both MoAb are directed against cell-surface antigens (Table I), which are not deposited extracellularly nor shed into the circulation. Furthermore, we included MoAb R24, which detected the glycolipid GD3 [3] and is to some extent subjected to a shedding process [4]. The method of macro-autoradiography was chosen in order to bridge the gap between microscopic examination and the low resolution techniques of, for example, scintigraphy or paired-label assay [5].

Manuscript received November 28, 1989; accepted for publication June 22, 1990.

Supported by the Deutsche Forschungsgemeinschaft, Sonderforschungsbereich 136 "Krebsforschung."

Reprint requests to: Dr. W. Tilgen, Universitäts-Hautklinik, Voss-Strasse 2, D-6900 Heidelberg, FRG.

Abbreviations:
MoAb: monoclonal antibody
HE: hematoxilin eosin
Bq: Becquerel

MATERIALS AND METHODS

Melanoma Cell Lines In Vitro and in Nude Mice Human melanoma cell lines were kindly provided by J. Fogh (MeWo, New York, NY) and S. Ferrone (Colo 38, Valhalla, NY). MML-I was established as described previously [6]. Cell lines were kept in RPMI 1640 media (GIBCO, Karlsruhe, West Germany) supplemented with 10% fetal calf serum, antibiotics, and 4 mMol glutamine (GIBCO). Malignant melanoma cells were detached from tissue-culture flasks by short treatment with 0.25% trypsin (Sigma, Munich, West Germany) containing 3 mMol EDTA, or by EDTA alone. Five million cells were inoculated subcutaneously into the flank of CD 1 nude mice (Charles River-WIGA, Sulzfeld, West Germany) and tumors reached a diameter of 7–20 mm after 2–5 weeks. During this time, animals were kept under barrier conditions.

Monoclonal Antibodies and Labeling The characteristics of MoAb used in this study are listed in Table I. M.2.9.4 was obtained from J. Brüggen and C. Sorg (Münster, FRG); R24 was obtained from W.G. Dippold (Mainz, West Germany). HD-Mel 3 was raised against the MML-I melanoma line by one of us [7]. A control

0022-202X/90/$03.50

Table I. Monoclonal Antibodies Used in the Study

MoAb	Isotype	Antigen	K[a]	Reference
M.2.9.4	IgG2a	gp 100	7.9×10^{8}[b]	[28]
HD-Mel 3	IgG2a	gp 95[c]	16.0×10^{8}[d]	
R24	IgG3	GD3	$<10^{8}$	[3]
HOPC-1	IgG2a	irrel.		

[a] Functional affinity constant.
[b] Affinity constant of $F(ab')_2$ fragments was 5.2×10^{8} l/M.
[c] W. Tilgen (unpublished).
[d] Affinity constants of $F(ab')_2$ and Fab fragments were 14.3×10^{8} and 6.0×10^{8} 1/M, respectively.

MoAb with irrelevant specificity (i.e., HOPC-1) was kindly donated by G. Hämmerling, Heidelberg. MoAb were purified from ascitic fluid by chromatography on Protein A and Mono Q columns (Pharmacia, Freiburg, FRG). Purity of preparations was checked by SDS polyacrylamide gel electroporesis. Labeling of antibodies with ^{125}I was carried out according to the IODO-GEN method [8]. Specific activities adjusted to 0.7–1.0 μCi/μg (26–37 kBq/μg) for M.2.9.4 and R24, and 2–5 μCi/μg (75–185 kBq/μg) for MoAb HD-Mel 3 and HOPC-1. These ranges were found to be secure with respect to conservation of the immunoreactivity of labeled MoAb as tested by the Lineweaver Burk method [9]. $F(ab')_2$ and Fab fragments were obtained by pepsin or papain digestion, respectively [10]. Fragments were purified by ion-exchange chromatography (see above) and tested for immunoreactivity. Only preparations with an immunoreactive fraction > 50% were used in animal experiments, regardless of whether this was intact IgG or fragments. Functional affinity constants [11] were determined by the Scatchard procedure, as modified by Trucco and de Petris [12].

Distribution of Labeled MoAb in Tumor-Bearing Nude Mice Mice (n = 4–6 per experimental group) received the labeled antibody preparation (30–70 μCi per animal) intravenously in a volume of 0.2 ml. In one experiment (Table II), the dose of MoAb HD-Mel 3 per animal was varied by admixture of the unlabeled MoAb to 70 μCi of labeled MoAb. At predetermined time points, animals were killed by extensive ether anesthesia. Mice were then pinned on a cork plate in prone position and frozen in dry ice-cooled isopentane and then in liquid nitrogen.

Preparation of Cryotome Sections and Autoradiography Liquid nitrogen-frozen mice were placed in a 250-ml plastic container and covered with methylcellulose gel (2.5% w/v in water), which was pre-cooled to 4°C. This immediately produced a frozen layer of methylcellulose around the mouse and prevented thawing of peripheral tissues. The frozen block (−20°C) was fixed on the pre-cooled support of the cryotome (Cambridge Instruments, previously Jung, Nussloch, FRG) with a small amount of methylcellulose gel. Whole-body sections were cut at the 20-μm setting and collected on an adhesive tape support. The sections were lyophilized for 3 h. Sections were counted in a gamma counter to gain an estimate of the time required for exposure on x-ray film (Kodak Xomatic AR). Exposure was calculated according to the counts per minute (cpm) of the sections as follows: days exposure = 100,000/cpm of section. Before placing sections on the x-ray film, adhesive parts of the sections were carefully dusted with talcum powder. After the calculated time, films were removed from the cassettes and were processed at 27°C in a Curix 242S automatic x-ray film processor (Agfa Gevaert, München, FRG).

Table II. Quantitative Densitometry of MoAb HD-Mel 3 Distribution in MML-I Xenografts[a]

MoAb/Fragment Injected	Amount μg per Mouse	Mean Signal In	
		Hot Spots	Cold Areas
IgG	10	1337 ± 120	466 ± 91
IgG[b]	110	683 ± 26	486 ± 18
IgG[b]	510	275 ± 7	226 ± 18
$F(ab')_2$[c]	22	1212 ± 173	339 ± 24
Fab[b]	27	1202 ± 208	452 ± 79

[a] Sections were produced from MML-I xenograft-bearing animals 12, 24, and 48 h after application of 70 μCi of ^{125}I-labeled HD-Mel 3 Fab, $F(ab')_2$, and intact IgG, respectively. The background signal of the films was 80–108 units.
[b] The injected dose of IgG was composed of 70 μCi of labeled MoAb plus the appropriate amount of unlabeled MoAb.
[c] Evaluation performed on tumors shown in Fig 3.

Computer-aided Densitometry of Autoradiograms This procedure has already been described in detail in a previous paper [13]. When an objective evaluation of film density was desired, a set of tissue-paste standards containing graded doses of ^{125}I [14] were co-exposed on the film. After scanning with a scanning densitometer (Joyce-Loebel), the digital density matrix was transformed into a "dose matrix" by virtue of the calibration curve obtained from tissue-paste standard readings. Such a matrix differs from a "radioactivity matrix" because of the finite range of electromagnetic radiation emitted by ^{125}I, which leads to a halo of film density surrounding a putative radioactive source. To acknowledge this fact, dose matrices were scaled in arbitrary units that are proportional to the radioactivity concentration per unit area. Two procedures were used for gathering information with relevance to the heterogeneity of radioactivity distribution, namely, establishment of linear dose profiles at given positions of dose matrices and region-of-interest integration of dose levels in selected areas. With the latter procedure, six regions of interest with a size of 10–20 pixels (25–50 μm^2) were evaluated in areas of high accumulation as well as in adjacent areas of low accumulation. The mean signal height of replicate regions of interest was averaged, thus yielding a parameter to describe representative dose levels in hot and cold areas of tumor sections.

Immunohistology In one set of experiments, MML-I tumors were excised 48 h after injection of ^{125}I-HD-Mel 3. Several series of consecutive standard cryotome sections (5 μm) were prepared and adjacent sections were subjected to autoradiography, to standard hematoxilin-eosin staining, or to immunohistology. With the latter method, target antigen expression was visualized by incubation of frozen sections with a 3.3 μg/ml solution of biotinylated MoAb HD-Mel 3 for 1 h. The detection system consisted of streptavidin-biotinylated peroxidase complex (Amersham, High Wycombe, UK) followed by a solution of 3-amino-9-ethylcarbazole (4 mg in 0.5 ml dimethylformamide) and H_2O_2 (30%, 5 μL) in 0.1 M sodium acetate buffer pH 5.0 (9.5 ml). After staining, sections were briefly rinsed with distilled water, counterstained with Mayer's hemalaun and mounted in glycerol/gelatine.

RESULTS

Non-uniform Distribution of MoAb in Melanoma Xenografts Because we used murine MoAb against human malignant melanoma-associated antigens, melanoma xenografts were the only tissues in nude mice to express the target antigen and, hence, to display specific accumulation of labeled MoAb (Figs 1*a,b*). In antigen-negative xenografts of non-melanoma origin tested with anti-melanoma MoAb, as well as in melanoma xenografts tested with MoAb of irrelevant sepcificity, only diffuse distribution patterns were observed, along with pools of radioactivity in peri-tumoral hemorrhages. Figure 1*d* shows a representative example out of a multitude of non-matching MoAb-tumor combinations tested. In the case of the specific MoAb R24, low affinity together with shedding of the target antigen resulted in a distribution pattern that was very similar to non-specific binding (Fig 1*c*). The patterns of radioactivity distribution observed with melanoma-specific and control MoAb are summarized in Table III. In the rest of the organism of melanoma-bearing nude mice, persistent radioactivity levels after application of intact IgG and fragments were noticed in the blood pool and the kidneys, respectively. In addition, low-molecular-weight degradation products (including iodide) gave a transient signal over the stomach and the urinary tract, the former being abrogated to some extent by blocking with perchlorate.

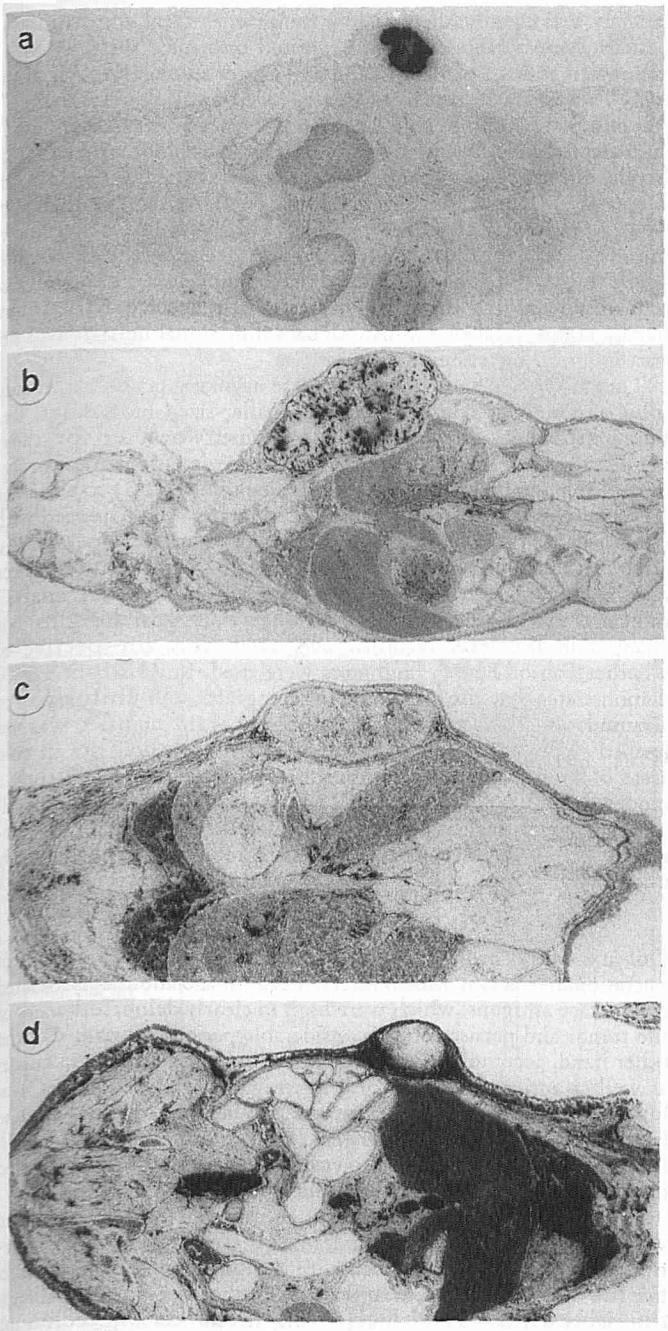

Figure 1. Typical distribution pattern of MoAb in melanoma xenografts. Whole-body autoradiographs performed 48 h after application of ^{125}I-labeled MoAb. *a*, M.2.9.4, F(ab')$_2$ fragments, MeWo xenograft; *b*, HD-Mel 3 MML-I xenograft; *c*, R24, Colo 38 xenograft; *d*, HOPC 1, MML-I xenograft. MoAb M.2.9.4 and HD-Mel 3 show specific reaction with melanoma xenografts MeWo and MML-I, respectively, both in vitro and in vivo. MoAb R24 is able to bind to Colo 38 melanoma cells in vitro (at 0°C [27]), but under *in vivo conditions* accumulation is weak and diffuse. Control MoAb HOPC 1 (irrelevant specificity) is not accumulated in MML-I melanoma xenografts.

The most interesting observation with respect to specific accumulation was that tracer doses of labeled MoAb — corresponding to doses used in diagnostic tumor targeting in patients — produced highly non-uniform accumulation patterns that depended on the melanoma line rather than on the MoAb used. One typical pattern was pronounced accumulation in the periphery of xenografts, as encountered in melanoma line MeWo accumulating M.2.9.4 (Fig 1*a*). The other typical pattern was accumulation in intra-tumoral foci as observed in MML-I xenografts accumulating HD-Mel 3 (Fig 1*b*).

Table III. Patterns of Radioactive MoAb Distribution in Melanoma and Non-Melanoma Xenografts – Summary

MoAb	Xenograft	Accumulation Pattern
Anti-Melanoma MoAb in Melanoma Xenografts		
M.2.9.4	MeWo	Periphery of nodule
HD-Mel 3	MML-I	Intra-nodular foci
R24	Colo 38	Weak, diffuse
Anti-Melanoma MoAb in Non-Melanoma Xenografts		
M.2.9.4	ASML[a]	Very weak, diffuse[b]
HD-Mel 3	ASML	Very weak, diffuse[b]
Control MoAb in Melanoma Xenograft		
HOPC 1	MML-I	Very weak, diffuse
HOPC 1	MeWo	Very weak, diffuse[b]

[a] Rat sarcoma [29] growing in the nude mouse; negative for melanoma-associated antigens.
[b] Autoradiografic images (not shown) that correspond closely to Fig 1*d*.

Influence of Necrosis and Antigen Expression The question was raised whether areas of very low MoAb accumulation coincided with necrosis and zones of low antigen expression or whether they were generated by limitations of accessibility. The extent of necrosis varied from one transplanted melanoma line to another, nodules with diameters below 7–10 mm being generally, but not always, devoid of macroscopic necrosis. When present, macroscopic necrosis showed transient and diffuse staining not exceeding the activity levels observed in the blood pool. However, this could by no means explain accumulation patterns as observed especially in MMl-I, i.e., discrete foci of active accumulation that are embedded in a matrix of "cold" tumor tissue (Fig 1*b*). To analyze this situation, we compared autoradiography, conventional HE staining, and immunohistology on neighboring sections of MML-I xenografts (Fig 2). It was found that the typical patchy pattern of radioactivity accumulation observed after injection of ^{125}I-HD-Mel 3 (Fig 2*b*) was paralleled by a virtually homogeneous distribution of the target antigen (Fig 2*a*). Control sections stained with sheep anti-mouse Ig showed a rim of immunoglobulin-positive murine cells around the xenograft nodules, but gave no indication of intra-tumoral foci of immunoglobulin accumulation (not shown). The most revealing observation was made on HE-stained sections adjacent to the sections processed by autoradiography, as hot spots in the latter coincided with micro-necrosis in the former (Fig 2*c*). When inspecting a series of sections, no difference in the frequency of patent microvessels was observed between necrotic and viable regions of MML-I tumor tissue. The absence of intra-tumoral foci of either high or low antigen expression in immunohistology (Fig 2*a*), as well as the absence of focal radioactivity accumulation of irrelevant MoAb (Fig 1*d*), led to the conclusion that the observed accumulation pattern could be explained neither by a corresponding pattern of antigen expression nor by unspecific trapping of external IgG in non-viable tissue.

An attempt was made to simultaneously visualize the blood supply of xenografts and MoAb deposition. ^{111}In-labeled erythrocytes were co-injected with ^{125}I-labeled MoAb and radioactivity levels were adjusted to yield an ^{111}In autoradiographic image (i.e., vessels, blood pools) immediately after preparation of sections and a ^{125}I image of MoAb distribution after decay of the ^{111}In tracer. However, no conclusive results were obtained because ^{111}In-erythrocytes showed up only the large vessels that were located primarily in the periphery of MeWo and throughout MML-I nodules. Besides this gross correspondence, no correlation was observed with individual areas of high MoAb accumulation, which may be nourished by small-sized tumor vessels that would go undetected by macro-autoradiography.

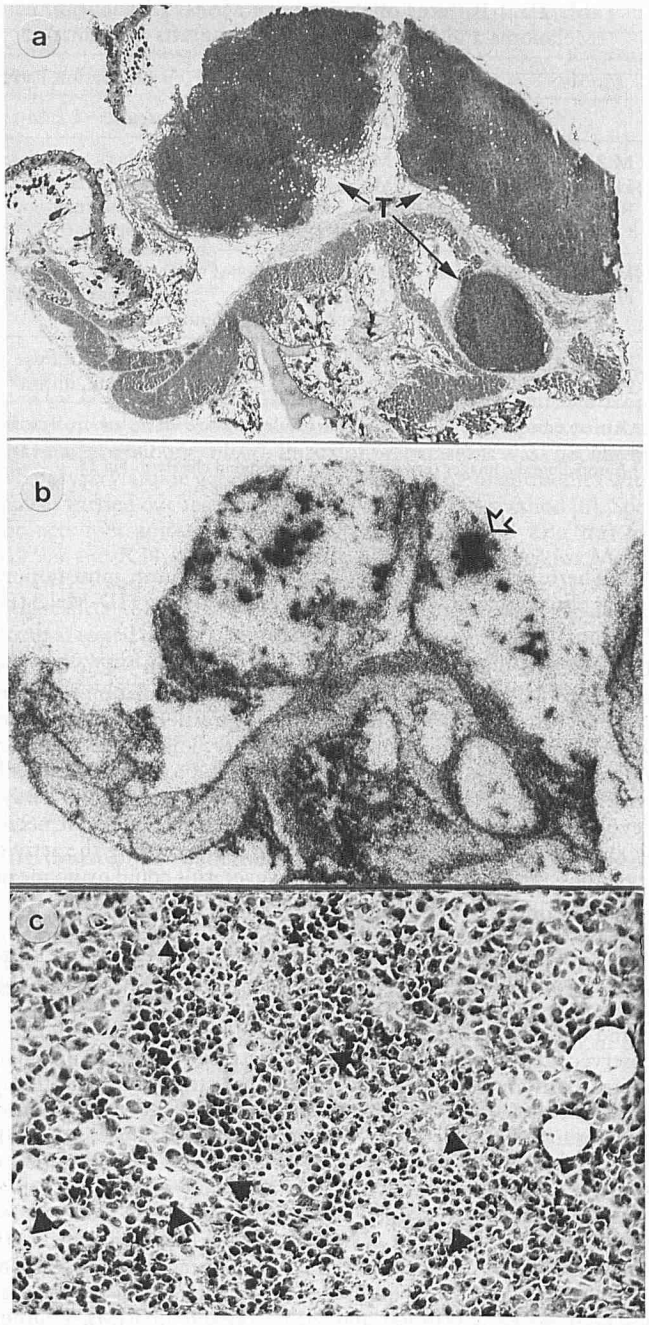

Figure 2. Non-uniformity of MoAb HD-Mel 3 accumulation in melanoma xenograft MML-I is not due to variations in the antigen expression. MoAb HD-Mel 3 was injected in a mouse bearing MML-I melanoma. After 48 h, the tumor was excised and sectioned on a conventional cryotome to achieve series of adjacent 5 μm sections. *a*, Detection of the target antigen by immunohistology using biotinylated HD-Mel 3 followed by streptavidin-biotinylated peroxidase complex. T, tumor nodules. *b*, detection of external MoAb accumulation by autoradiography. *c*, detection of necrosis by staining with hematoxilin/eosin. The sections show the area corresponding to a hot spot in *b (arrow)*. Necrotic foci are marked by *arrowheads*. *a,b*, magnification ×17; *c*, magnification ×112.

Intra-tumoral Distribution of Intact IgG versus Fragments

With respect to a therapeutic application of MoAb conjugates, it is of paramount interest to achieve uniformity, if not saturation, of tumor uptake. One of the approaches that proved to be successful in MeWo transplants was MoAb dose escalation. This led to a gradual filling up of the central part of nodules [15]. To see whether the strategy was equally effective in a tumor with focal accumulation pattern, MoAb HD-Mel 3 was injected into mice with MML-1 xenografts at doses of 10, 110 and 510 μg per animal. MoAb distribution was characterized by computer-aided densitometry and analysis of signal heights in regions of interest placed over hot spots and cold areas of dose matrices. As can be seen in Table II, mean signal height differences were highly pronounced at the tracer dose but decreased with increasing doses of (unlabeled) MoAb. At the dose of 510 μg per animal, the difference was virtually leveled off, indicating a saturation of antigenic sites even in areas that were not reached by the tracer dose. It has to be noted that because dose escalation was achieved by adding increasing amounts of unlabeled MoAb to a fixed amount of labeled MoAb, the absolute signal height was decreasing with increasing dose.

The alternative approach to increase antibody penetration into solid tumor tissue consists of using smaller-sized molecules, i.e., fragments. Again, computer-aided densitometry was used for studying distribution patterns, now applying the region of interest procedure (Table II) and linear-dose profile calculation (Fig 3) to the same set of sections. Mice bearing MML-I xenografts were injected with either Fab or $F(ab')_2$ fragments and autoradiograms were performed after 12 h and 24 h, respectively, according to the different clearance rates associated with both types of fragments. Computer analysis indicated neither major changes in the peak signal heights nor changes in the level recorded over cold areas, irrespective of whether Fab or $F(ab')_2$ fragments were used. In addition, Fig 3c demonstrates that also with MeWo xenografts, non-uniformity of accumulation, in this case in the periphery of the nodule, was not leveled off by the use of fragments. When signal heights in cold areas of the tumors were compared to those of normal tissues, a moderate increase was recorded with fragments (data not included) especially with Fab, indicating that penetration was indeed facilitated, yet in a way that left peak-to-background ranges essentially unchanged.

DISCUSSION

Our autoradiographic data highlighted the targeting potential of operationally specific MoAb directed against melanoma-associated cell surface antigens, which were high in clearly delimited areas of the tumor and persisted for a considerable period of time. On the other hand, accumulation of irrelevant MoAb in melanoma tissue, as well as anti-melanoma MoAb in antigen-negative tumors, was low, transient, and confined to necrotic or hemorrhagic areas. The latter finding may reflect a slower clearance of non-bound MoAb from these areas, as compared to viable tissue, as has been suggested in colon carcinoma xenografts in the hamster [16,17].

Distinct patterns of radioactivity accumulation were observed with anti-melanoma MoAb. Predominant accumulation in the periphery of nodules was observed with MoAb M.2.9.4 in melanoma line MeWo. The same pattern was previously observed with differently labeled M.2.9.4 [18], thus proving that the labeling technique did not influence the distribution pattern. Accumulation in an array of intra-tumoral foci was observed with HD-Mel 3 in melanoma line MML-I. MoAb R24, which binds with low functional affinity to a glycolipid antigen that is subject to shedding [4], showed a distribution pattern similar to non-specific MoAb.

An important question was whether positive MoAb accumulation reflected the presence of viable melanoma tissue and whether spared areas corresponded to necrosis. Preferential uptake in the periphery was also observed in small nodules of melanoma line MeWo, which were devoid of macroscopic necrosis. When increasing the MoAb dose injected, an increasingly uniform radioactivity distribution was observed in this melanoma line [15], suggesting that "cold" areas could indeed be targeted, provided the input concentration of MoAb was high enough. Hence, it was unlikely that the MoAb accumulation pattern observed in MeWo simply reflected the presence of viable, antigen-positive melanoma cells in the periphery of nodules only. With the MML-I type of melanoma xenografts exhibiting a patchy accumulation within the nodule, it was evident beforehand that the nodules would not consist of a

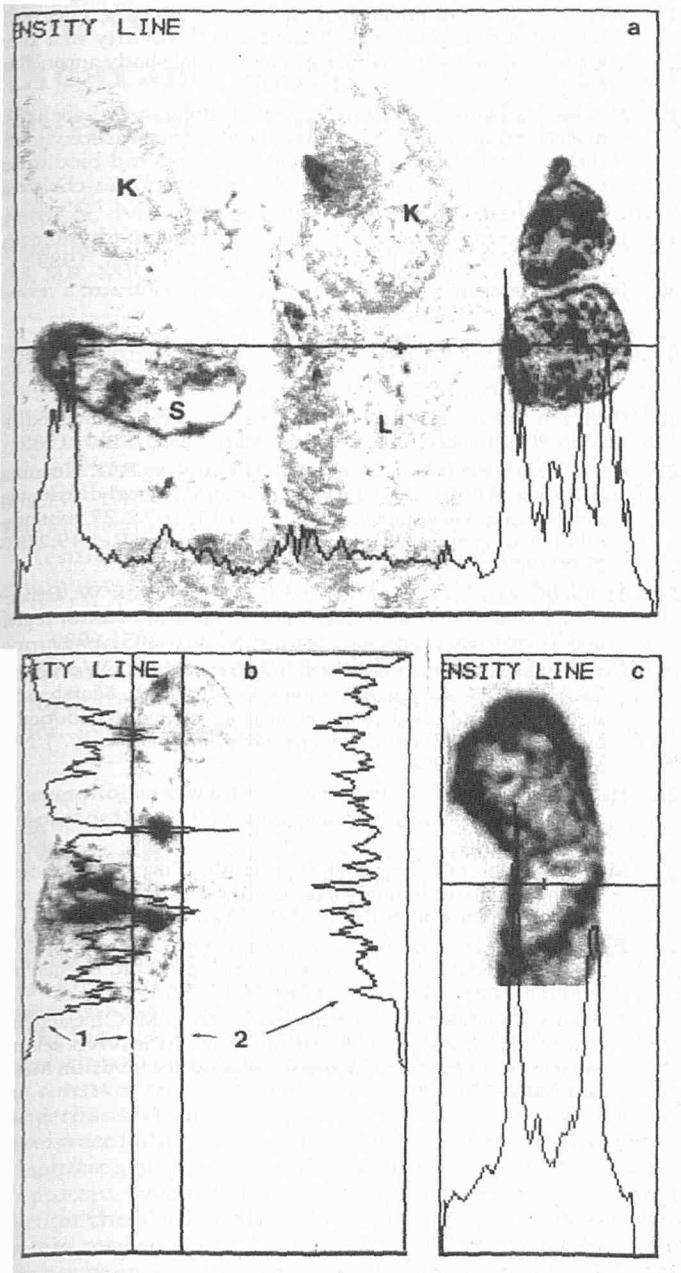

Figure 3. Computer-aided densitometry of autoradiographs obtained with MoAb fragments. *a*, Dose matrix and profile through tumor and body of a mouse with MML-I transplant 24 h after application of $F(ab')_2$ from HD-Mel 3; *b*, dose matrix and two profiles through a MML-I transplant 12 h after application of HD-Mel 3 Fab. The *left hand profile #1* highlights radioactivity distribution in a non-uniformly accumulating area of the section along *straight line #1* whereas the *right hand profile #2* displays the radioactivity distribution along *straight line #2* in an area with seemingly uniform radioactivity distribution; *c*, dose matrix and profile through a MeWo transplant 24 h after application of $F(ab')_2$ from M.2.9.4 Preferential accumulation in the periphery of nodule is observed with the fragment as it is the case with intact IgG.

predominantly necrotic mass with interspersed nests of viable tumor cells. This was confirmed by histologic analysis of adjacent sections, which showed nodules composed of a compact mass of melanoma cells with virtually uniform antigen expression. Nevertheless, antibody accumulation did not follow the presence of the antigen. At higher magnification, micro-necrosis was detected in HE-stained neighboring sections. The localization of necrotic foci corresponded exactly to that of hot spots in the autoradiographs.

The dichotomy of peripheral versus focal accumulation may be a consequence of peripheral versus central vascularization [19]. In addition to peripheral vascularization, a gradient of the interstitial pressure from the center to the outer part of the nodule [19,20] may result in a reduction of both blood flow and convectional extravasation in the central part and result in net flow of interstitial fluid to the periphery [21]. Both factors would act in the same direction, thus deflecting MoAb access and retention to the outer part of the tumor. With respect to the situation encountered in MML-I melanoma xenografts, it is suggested that extravasation is hindered by a fairly tight blood-tissue barrier that may be disturbed by micro-necrosis, thus facilitating extravasation irrespective of molecular size [22].

In a recent paper by del Vecchio et al [23], autoradiographic studies were performed with melanoma tissue specimen from patients after injection of ^{131}I-labeled MoAb 9.2.27. Results were strikingly similar to those obtained in our study, in that radioactivity accumulation was highly heterogeneous with peak-to-background ratios up to 17:1, whereas antigen expression was homogeneous. In two of six patients, a pattern of high-intensity focal accumulation was found that is clearly reminiscent of the pattern obtained with MML-I xenografts. Foci were located in the vicinity of a vessel, suggesting that the permeability barrier was generally intact and that exceptional conditions were required for extravasation to occur. An additional parallelism was observed in a nodule with a central necrosis, where radioactivity accumulation took place predominantly in the periphery. This concordance of findings demonstrates that meaningful investigations with respect to melanoma targeting can indeed be carried out in nude mouse models.

According to previously reported data [15] and to data now collected with the MML-I melanoma line, both types of non-uniformity in MoAb distribution could be leveled off by application of increasing doses of MoAb. This is not a trivial finding, because we identified one tumor model, i.e., the BJAB human B-lymphoma in which dose escalation did not suffice for achieving quasi-uniformity of MoAb uptake [24]. The importance of the finding relates to therapeutic approaches that rely on the premise of hitting every single tumor cell in a solid tumor nodule. But also in diagnostic tumor targeting dose escalation has been reported to yield better signals [25].

With respect to MoAb fragments, the general finding was that $F(ab')_2$ and Fab produced the same type of accumulation pattern as intact MoAb, i.e., peak-to-background ratios were high. On the other hand, Fab-associated radioactivity levels in the cold areas of melanoma nodules were higher than levels in most normal tissues, suggesting that an augmented uptake of smaller molecules could well be achieved if the rapid clearance of these fragments from the blood could be counteracted. There is indeed data to support such an assertion [26]. Whether the monovalency of Fab, as opposed to the divalency of $F(ab')_2$ and IgG, may influence the depth of penetration into antigen-positive tissue could only be judged from a larger panel of Fab species, although this approach will meet limitations due to the low functional affinity of most Fab preparations.

We would like to thank H. Kirchgessner for expert technical assistance. The generous gift of monoclonal antibodies by Drs. C. Sorg, J. Brüggen, G. Hämmerling, and W.G. Dippold is gratefully acknowledged.

REFERENCES

1. Larson B, Ullberg S: Whole-body autoradiography. J Histochem Cytochem 29:216–225, 1981
2. Matzku S, Brüggen J, Bröcker EB, Sorg C: Criteria for selecting monoclonal antibodies with respect to accumulation in melanoma tissue. Cancer Immunol Immunother 24:151–157, 1987
3. Pukel CS, Lloyd KO, Travassos LR, Dippold WG, Oettgen HF, Old LJ: GD3, a prominent ganglioside of human melanoma. Detection and characterization by mouse monoclonal antibody. J Exp Med 155:1133–1147, 1982

4. Bernhard H, Meyer zum Büschenfelde K-H, Dippold WG: Ganglioside GD3 shedding by human malignant melanoma cells. Int J Cancer 44:155–160, 1989
5. Pressman D, Day ED, Blau M: The use of paired labeling in the determination of tumor-localizing antibodies. Cancer Res 17:845–850, 1957
6. Tilgen W, Dzarlieva RT, Breitkreutz D, Hennes B, Engstner M, Matzku S, Fusenig N: Heterogeneity of human malignant melanoma cells in vivo and in vitro: role of experimental systems. In: Bagnara J, Klaus SN, Paul E, Schartl M (eds.): Pigment Cell 1985. Biological, molecular, and clinical aspects of pigmentation. University of Tokyo Press, Tokyo, 1985, pp 435–447
7. Tilgen W, Matzku S: Antibody-mediated modulation of melanoma-associated antigens: access of monoclonal antibodies into melanoma cells and melanoma tissue. In: Ferrone S (ed.): Human Melanoma: From Basic Research to Clinical Applications. Springer-Verlag, Heidelberg, 1990, pp 119–132
8. Fraker PJ, Speck JC: Protein and cell membrane iodinations with a sparingly soluble chloroamide, 1,3,4,6-tetrachloro-3α,6α-diphenylglycoluril. Biochem Biophys Res Commun 80:849–857, 1980
9. Matzku S, Kirchgessner H, Dippold WG, Brüggen J: Immunoreactivity of monoclonal anti-melanoma antibodies in relation to the amount of radioactive iodine substituted to the antibody molecule. Eur J Nucl Med 11:260–264, 1985
10. Parham P, Androlewicz MJ, Brodsky FM, Holmes NJ, Ways JP: Monoclonal antibodies: Purification, fragmentation and application to structural and functional studies of class I MHC antigens. J Immunol Meth 53:133–173, 1982
11. Hornick CL, Karush F: Antibody affinity. III. The role of multivalence. Immunochemistry 9:325, 1972
12. Trucco M, de Petris S: Determination of equilibrium binding parameters of monoclonal antibodies specific for cell surface antigens. In: Lefkovits I, Pernis B (eds.). Immunological Methods. Academic Press, New York, 1981, pp 1–26
13. Schmid U, Bihl H, Matzku S: Antibody accumulation in small tissue samples: assessment by quantitative autoradiography. Nucl Med Biol (in press)
14. Clark CR, Hall MD: Hormone receptor autoradiography: recent developments. TIBS 11:195–199, 1986
15. Matzku S, Kirchgessner H, Schmid U, Temponi M, Ferrone S: Melanoma targeting with a cocktail of monoclonal antibodies to distinct determinants of the human HMW-MAA. J Nucl Med 30:390–397, 1989
16. Fand I, Sharkey RM, McNally WP, Brill AB, Som P, Yamamoto K, Primus FJ, Goldenberg DM: Quantitative Whole-Body Autoradiography of Radiolabeled Antibody Distribution in a Xenografted Human Cancer Model. Cancer Res 46:271–277, 1986
17. Fand I, Sharkey RM, Primus FJ, Cohen SA, Goldenberg DM: Relationship of radioantibody localization and cell viability in a xenografted human cancer model as measured by whole-body autoradiography. Cancer Res 47:2177–2183, 1987
18. Matzku S, Schuhmacher J, Kirchgessner H, Brüggen J: Labeling of monoclonal antibodies with a 67Ga-phenolic aminocarboxylic acid chelate. Part II. Comparison of immunoreactivity and biodistribution of monoclonal antibodies labeled with the 67Ga-chelate or with 131I. Eur J Nucl Med 12:405–412, 1986
19. Jain RK: Delivery of novel therapeutic agents in tumors: physiological barriers and strategies. J Natl Cancer Inst 81:570–576, 1989
20. Jain RK: Transport of molecules in the tumor interstitium: a review. Cancer Res 47:3039–3051, 1987
21. Butler TP, Grantham FH, Gullino PM: Bulk transfer of fluid in the interstitial compartment of mammary tumors. Cancer Res 35:3084–3088, 1975
22. Cobb LM: Intratumor factors influencing the access of antibody to tumor cells. Cancer Immunol Immunother 28:235–240, 1989
23. Del Vecchio S, Reynolds JC, Carrasquillo JA, Blasberg RG, Neumann RD, Lotze MT, Bryant GJ, Farkas RJ, Larson SM: Local distribution and concentration of intravenously injected 131I-9.2.27 monoclonal antibody in human malignant melanoma. Cancer Res 49:2783–2789, 1989
24. Trauth BC, Klas C, Peters AMJ, Matzku S, Möller P, Falk W, Debatin K-M, Krammer PH: Monoclonal antibody-mediated tumor regression by induction of apoptosis. Science 245:301–305, 1989
25. Carrasquillo JA, Abrams PG, Schroff RW, Reynolds JC, Woodhouse CS, Morgan AC, Keenan AM, Foon KA, Perentesis P, Marshall S et al: Effect of antibody dose on the imaging and biodistribution of indium-111 9.2.27 anti-melanoma monoclonal antibody. J Nucl Med 29:39–47, 1988
26. Halpern SE, Dillman RO: Problems associated with radioimmunodetection and possibilities for future solutions. J Biol Response Mod 6:235–262, 1987
27. Matzku S, Bröcker EB, Brüggen J, Dippold WG, Tilgen W: Modes of binding and internalization of monoclonal antibodies to human melanoma cell lines. Cancer Res 46:3848–3854, 1986
28. Brüggen J, Bröcker EB, Suter L, Redmann K, Sorg C: The expression of tumor-associated antigens in primary and metastatic human malignant melanoma. Behring Inst Mitt 74:19–22, 1984
29. Matzku S, Komitowski D, Mildenberger M, Zöller M: Characterization of BSp73, a spontaneous rat tumor and its in vivo selected variants showing different metastasizing capacities. Invasion Metastasis 3:109–123, 1983